Supporting Information

Aubin-Tam et al. 10.1073/pnas.0807299106

SI Text

Molecular Dynamics Simulations with Explicit Solvent. MD simulations were performed with TIP3P explicit solvent on D50C-NP and K99C-NP. Internal water molecules in the crystal were kept in the structure. The NP-cyt *c* conjugate was centered in a sphere containing water molecules (80 Å in diameter). Water molecules whose oxygen atom is closer to the heavy atom by <2.8 Å were deleted. The deformable boundary potential for this sphere was obtained from the MMTSB server (1, 2). Outside of the sphere, water molecules were subjected to Langevin dynamics with a friction coefficient of 5 ps^{-1}. After solvation, there were 6,907 water molecules for the D50C-NP system and 6,944 water molecules for the K99C-NP system. Each BPS molecule was carrying a charge of $-4e$. A 12-Å cutoff was applied for nonbonded interactions with a switch function between 8 Å and 12 Å. Molecules within 13 Å were included in the nonbonded list. After energy minimization, the system was heated from 48 K to 450 K for 80 ps with C_α atoms harmonically constrained. It was then equilibrated at 450 K for 100 ps. Leap-frog dynamics trajectories were carried out with 2-fs time steps for 4.5 ns and the SHAKE algorithm was used to constrain bonds involving hydrogen atoms. The list of nonbonded interaction pairs was updated every 5 steps.

1. Brooks CL III, Karplus M (1983) Deformable stochastic boundaries in molecular dynamics. *J Chem Phys* 79:6312–6325.
2. Brunger A, Brooks CL III, Karplus M (1984) Stochastic boundary conditions for molecular dynamics simulations of ST2 water. *Chem Phys Lett* 105:495–500.
3. Bixler J, Bakker G, McLendon G (1992) Electrochemical probes of protein folding. *J Am Chem Soc* 114:6938–6939.
4. Tezcan FA, Winkler JR, Gray HB (1998) Effects of ligation and folding on reduction potentials of heme proteins. *J Am Chem Soc* 120:13383–13388.
5. Frishman D, Argos P (1995) Knowledge-based protein secondary structure assignment. *Proteins* 23:566–579.
6. Humphrey W, Dalke A, Schulten K (1996) VMD—Visual molecular dynamics. *J Mol Graphics* 14:33–38.

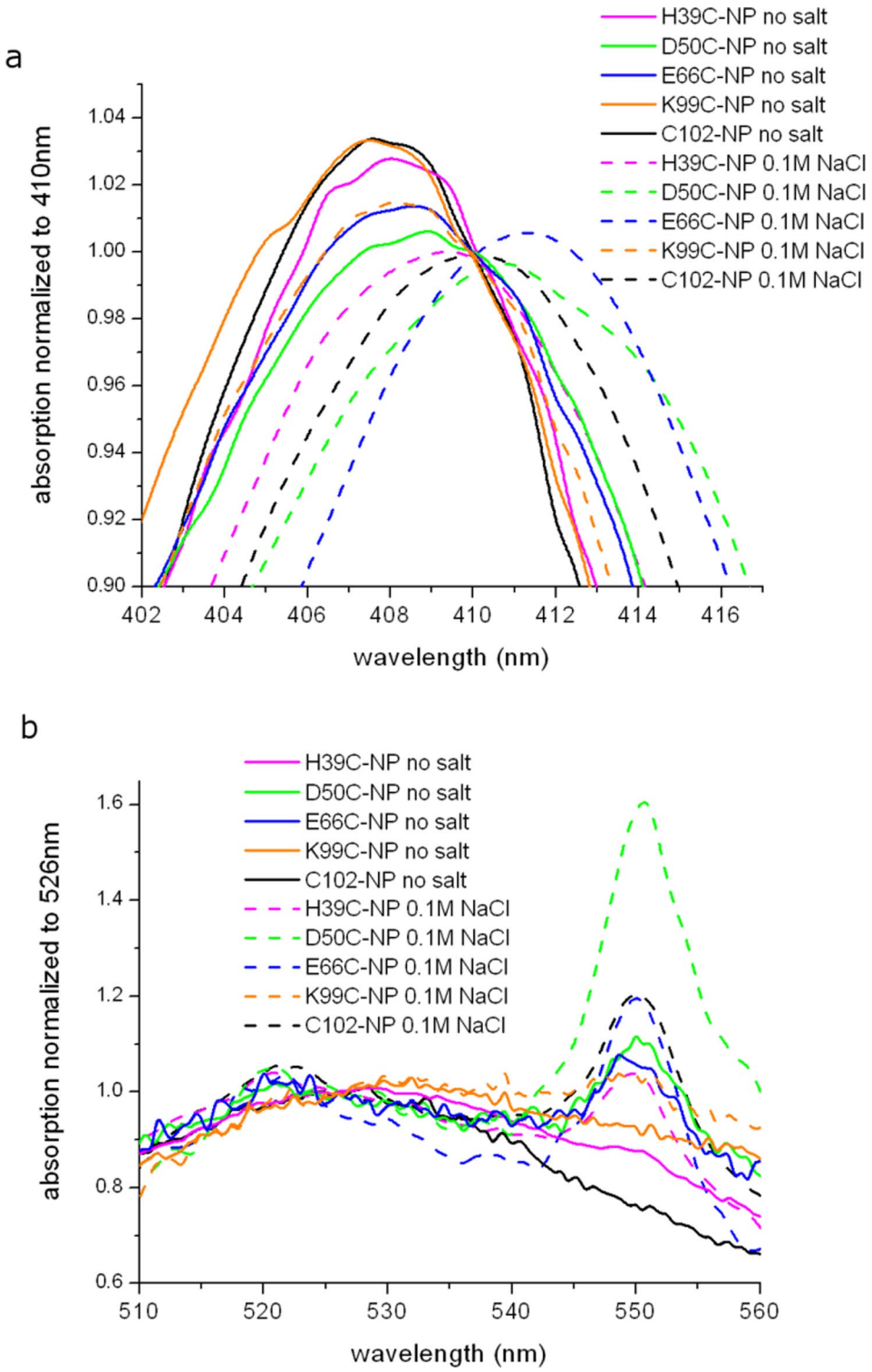

Fig. S1. Soret (*a*) and Q-band (*b*) absorption of conjugates with and without 0.1 M NaCl. NP contribution to the spectra has been subtracted. For easier comparison between spectra, the data have been normalized to absorption at 410 nm (*a*) and 526 nm (*b*), which have a molar extinction coefficient independent of the heme oxidation state. When cyt *c* unfolds, it is known that its redox potential decreases, thus the heme is more readily oxidized (3, 4). Here, the heme is partially reduced in several conjugates (D50C-NP and E66C-NP without salt and all conjugates with 0.1 M NaCl), indicating retained protein redox activity because it can still exchange electrons.

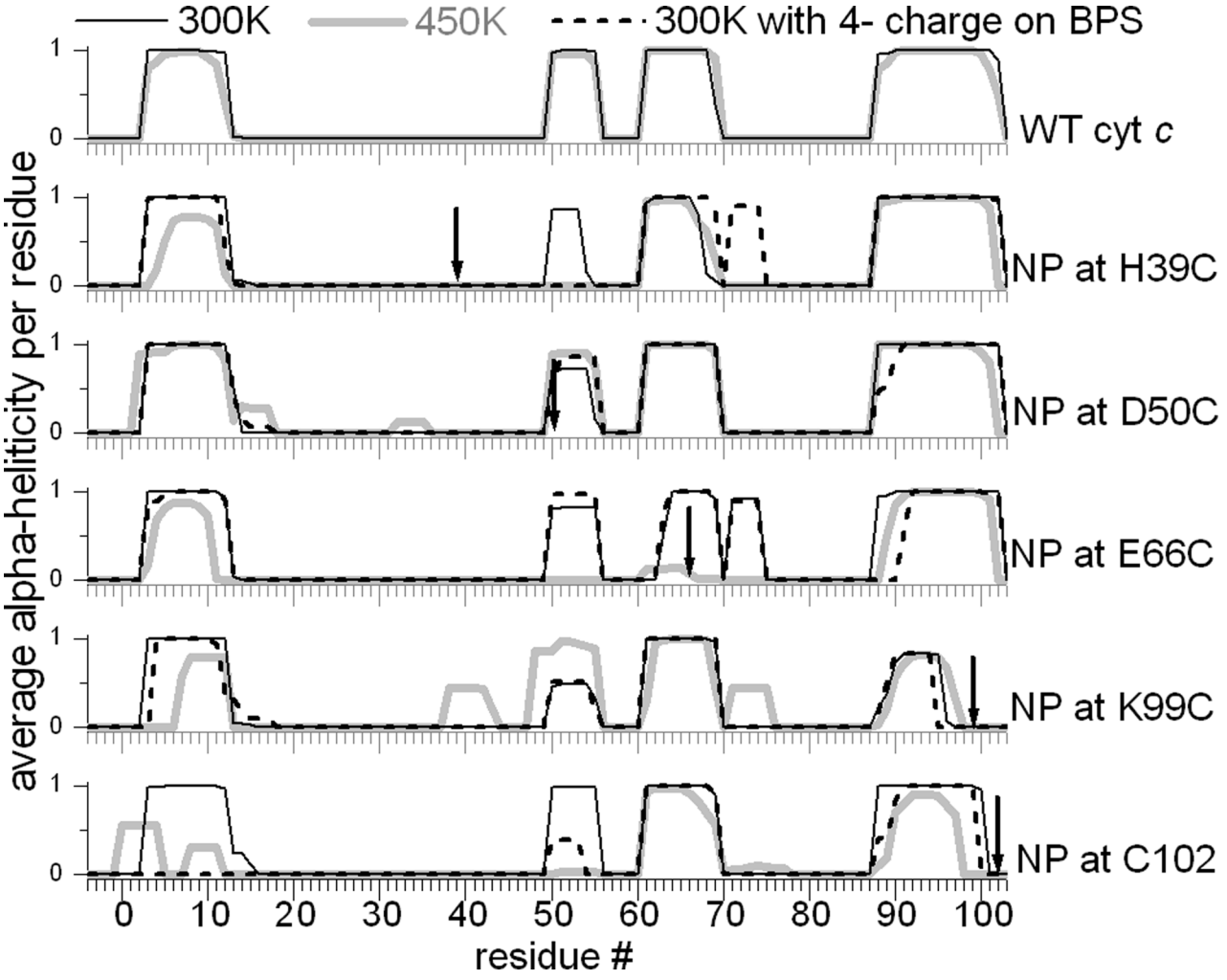

Fig. S2. Comparison of α-helicity. Secondary structure is determined by using STRIDE (5) and averaged over the last 500 ps of simulations at 300 K, at 450 K with normal charges on BPS, and at 300 K with the charges of BPS molecules increased from $-2e$ to $-e$. Arrows: NP labeling sites. While the short 70's helix is not recognized by STRIDE in the WT at 300 K, its presence is confirmed by the H bond between P71 and I75 (see Fig. S3).

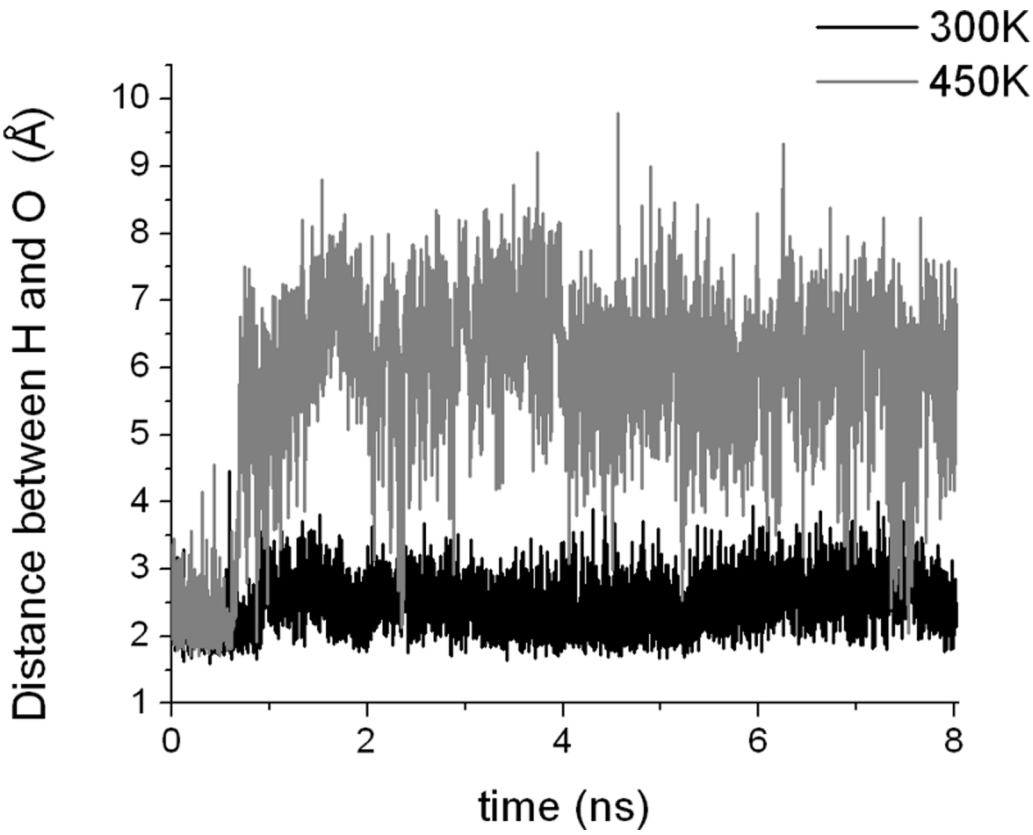

Fig. S3. H bond between P71 and I75 in 70's helix of WT without NP. The distance between the O of P71 and the H of I75 is plotted along the MD trajectory at 300 K (black) and 450 K (gray).

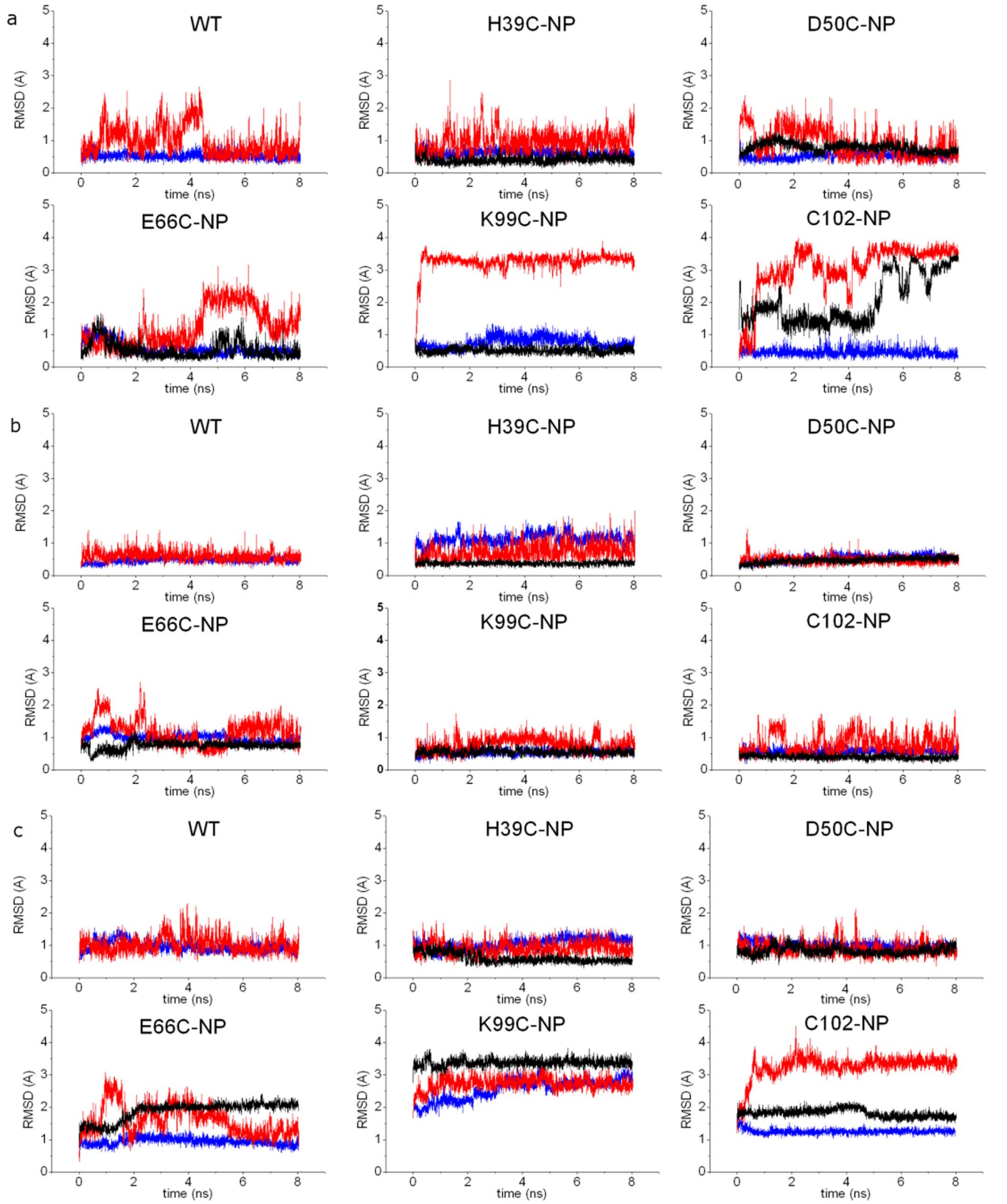

Fig. S4. rmsd profile of C_α of N-terminal (*a*), 60's (*b*), and C-terminal (*c*) α-helices of conjugates, from the energy minimized WT crystal structure at 300 K (blue), at 450 K (red), and at 300 K with charges enhanced on BPS (black).

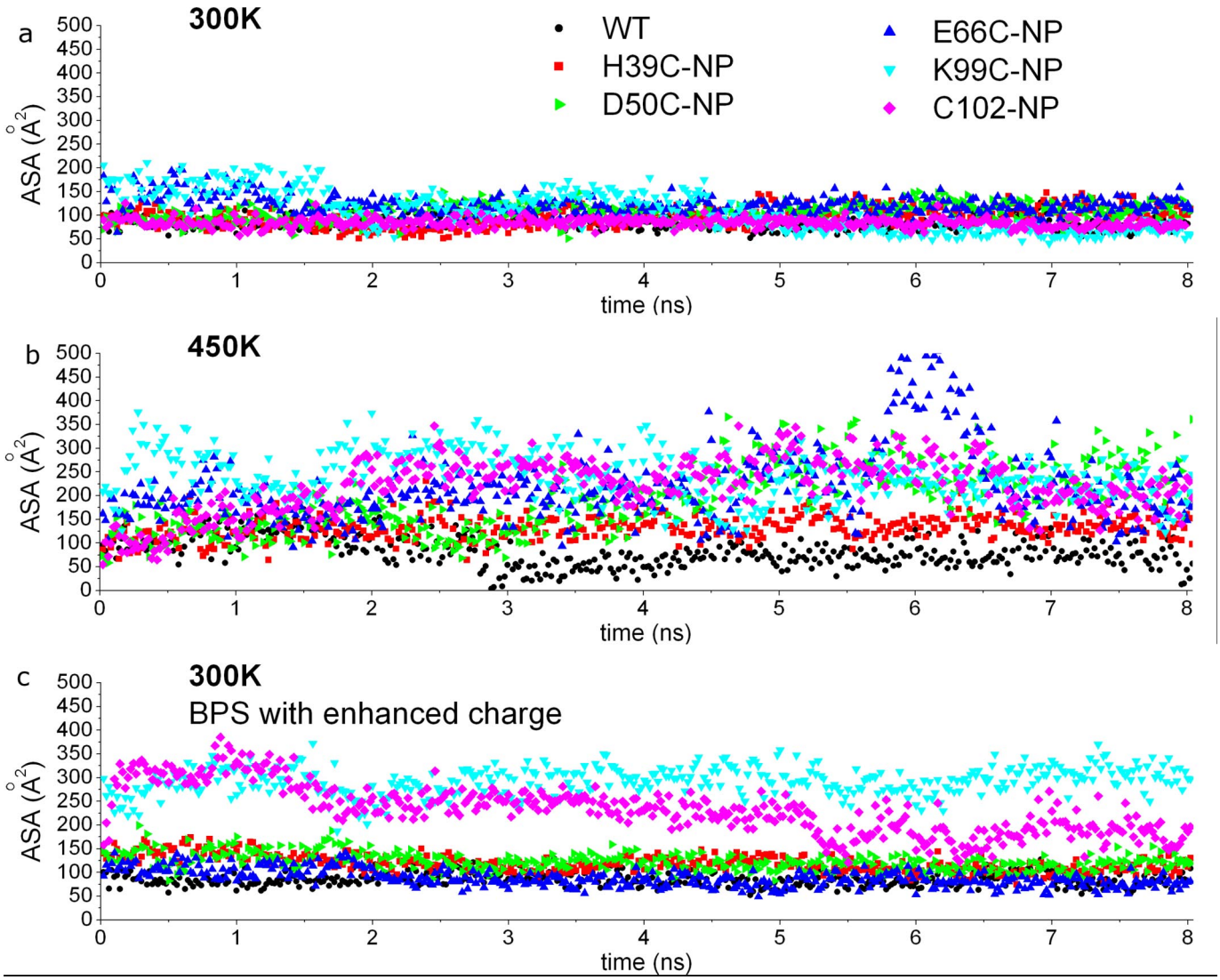

Fig. S5. Solvent-accessible surface area (ASA) of the side chains of Leu-9, Phe-10, Leu-94, Tyr-97, and Leu-98, which are part of the hydrophobic cluster of the N–C foldon. ASA profiles are calculated by using a probe sphere with a radius of 1.4 Å. (*a*) At 300 K, (*b*) at 450 K, and (*c*) at 300 K with charges enhanced on BPS.

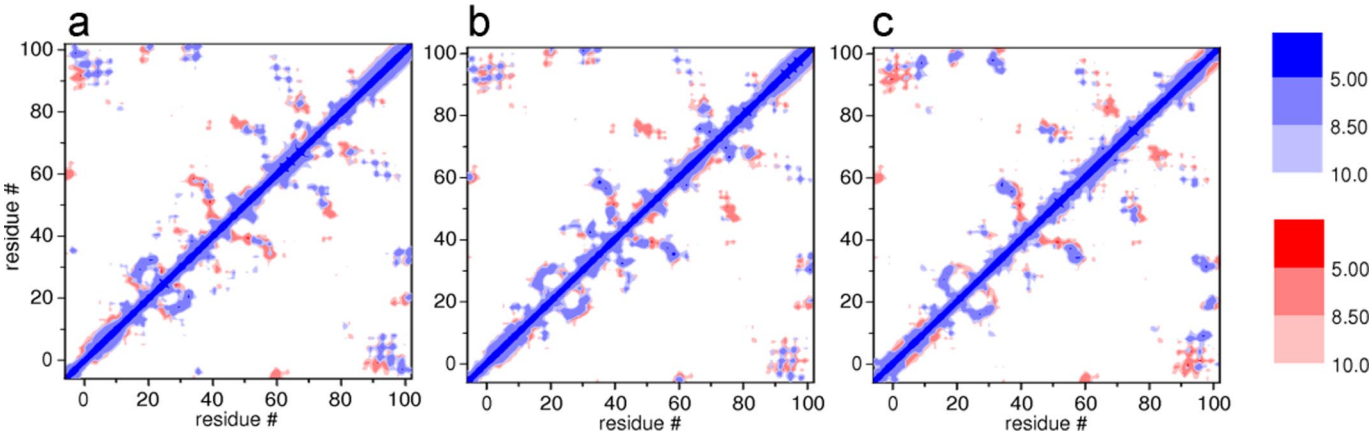

Fig. S6. Contact map of H39C-NP (*a*), E66C-NP (*b*), and C102-NP (*c*). The distance between C_α atoms (red, WT; blue, NP conjugate) is averaged over the last 500 ps of simulation at 450 K.

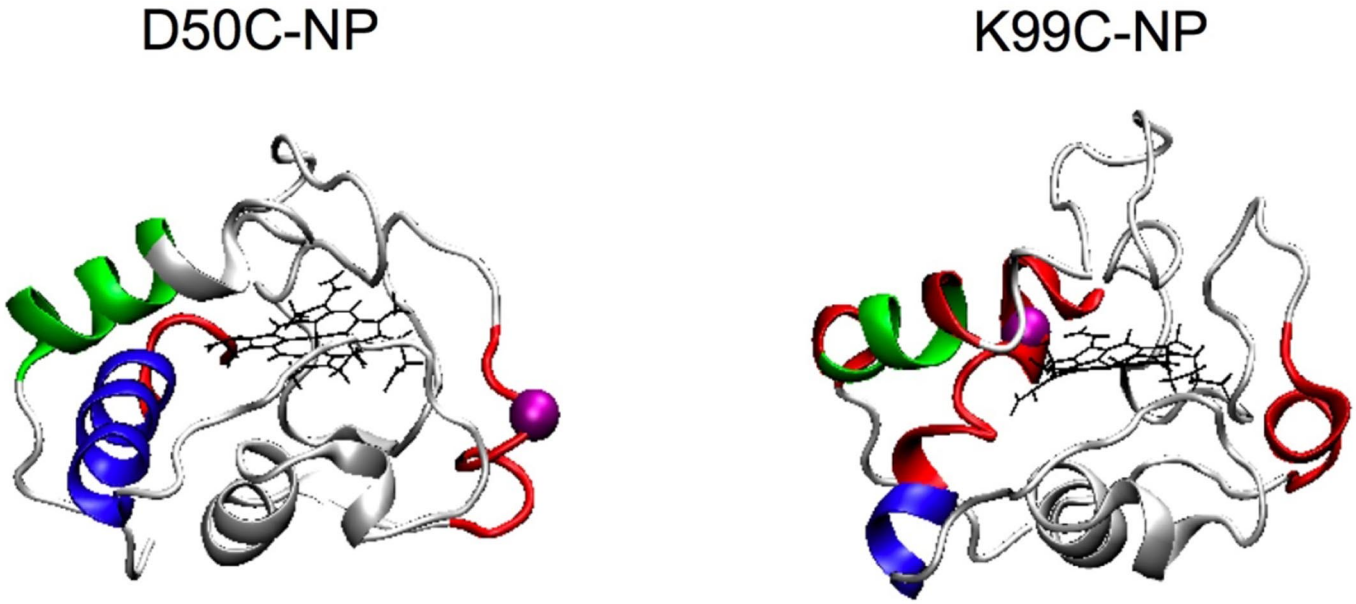

Fig. S7. Snapshot of protein structure at the end of 4.5-ns MD simulations at 450 K with explicit solvent and double charges on BPS. Green/blue, N-/C-terminal helices; red, loss of >50% α-helicity from WT structure; purple sphere, NP attachment site. The program VMD was used for visualization (6). See also Fig. 4.

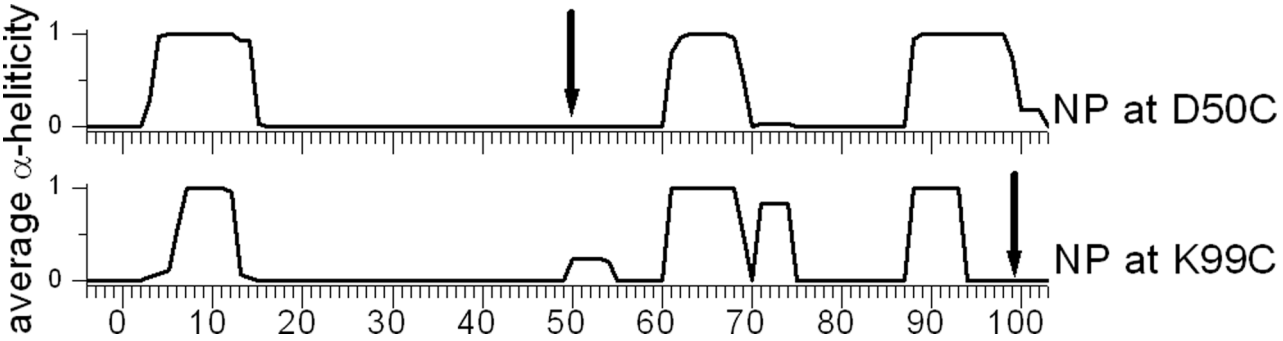

Fig. S8. Comparison of α-helicity for explicit solvent simulations. Secondary structure is determined by using STRIDE (5) and averaged over the last 500 ps of simulations. Arrows: NP labeling sites.

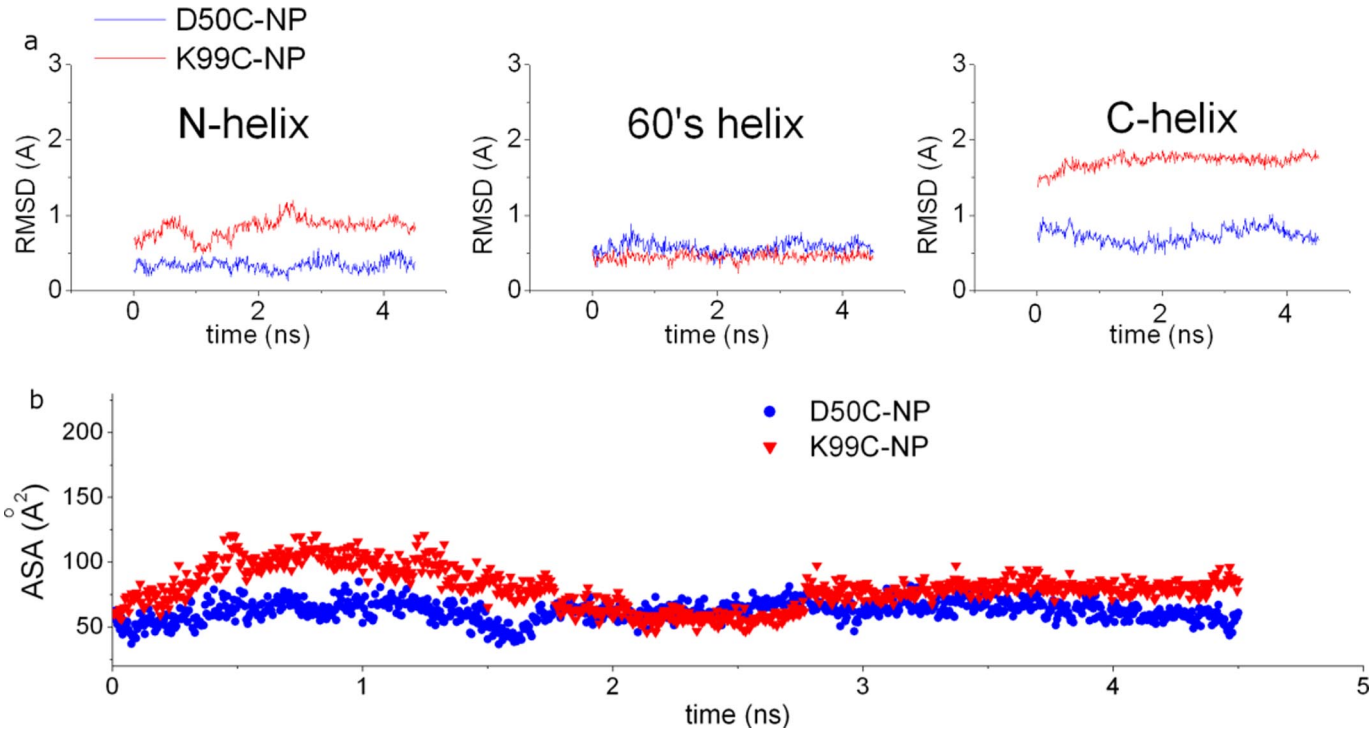

Fig. S9. Trajectory analysis of explicit water simulations. (*a*) rmsd profile of C_α of N-terminal, 60's and C-terminal α-helices of conjugates from energy minimized WT crystal structure. (*b*) ASA profile of the side chains of Leu-9, Phe-10, Leu-94, Tyr-97, and Leu-98 for explicit solvent simulations of D50C-NP (blue) and K99C-NP (red).

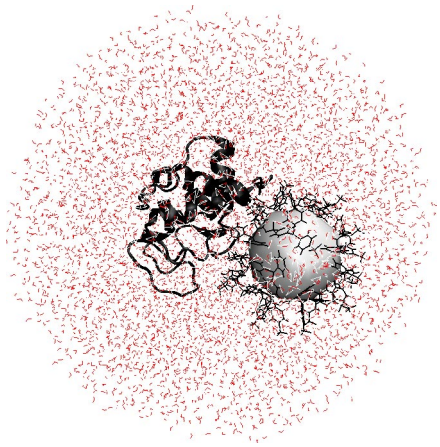

Fig. S10. Protein–NP conjugate in an 80-Å-diameter TIP3P water sphere.